SSCL-268

SSCL-268

Superconducting Super Collider Laboratory

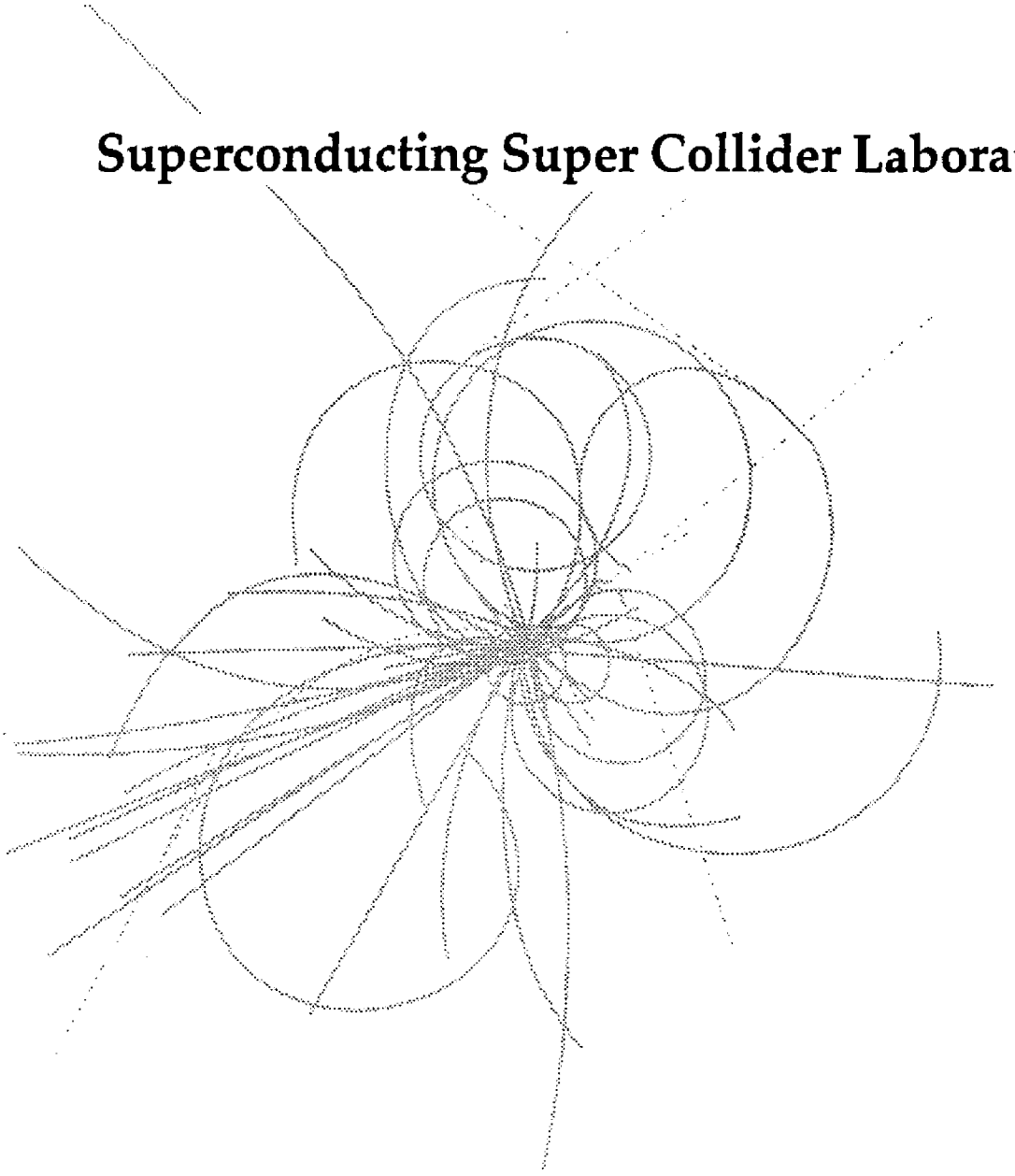

Numerical Studies of the SSC Injection Process: Long Term Tracking

T. Garavaglia, S. Kauffmann, R. Stiening, and D. Ritson

April 1990

SSCL-268

NUMERICAL STUDIES OF THE SSC INJECTION PROCESS: LONG TERM TRACKING*

T. Garavaglia, S. K. Kauffmann,
R. Stiening, and D. M. Ritson

Superconducting Super Collider Laboratory†
Accelerator Division
2550 Beckleymeade Avenue
Dallas, TX 75237

April 1990

* Presented at the International Industrial Symposium on the Super Collider, Miami Beach, Florida, March 14–16, 1990.

† Operated by the Universities Research Association, Inc., for the U.S. Department of Energy under Contract No. DE-AC02-89ER40486.

NUMERICAL STUDIES OF THE SSC INJECTION PROCESS: LONG TERM TRACKING

T. Garavaglia, S. K. Kauffmann, R. Stiening, and

D. M. Ritson

Superconducting Super Collider Laboratory*

2550 Beckleymeade Avenue, Dallas, TX 75237

Abstract

Results are presented for tracking protons within the Superconducting Super Collider during the injection phase for up to seven million turns. The results for the 4 cm and the 5 cm aperture machines are compared. X and y invariant amplitude and phase space information are given which are characteristic of bounded chaotic motion. The present long term tracking results were obtained using SSCTRK for groups of four particles started at four different equally spaced injection points on eight different machines, each characterized by a different random seed. A qualitative interpretation of the dynamical behavior of the protons is given in terms of some simple models using nonlinear differential equations.

INTRODUCTION

SSCTRK was developed by D. M. Ritson to address the question of the dynamical behavior of the proton beams in the Superconducting Super Collider (SSC) during the injection period. Long term tracking studies where initiated using SSCTRK in late 1989 in order to determine the suitability of the 4 cm magnetic aperture design. As a result of these and related studies decisions were made to recommend a change in the basic design of the Collider so that the magnetic aperture would be increased to 5 cm. Defining bounded chaotic

* Operated by Universities Research Association, Inc., for the U.S. Department of Energy under Contract No. DE-AC02-89ER40486.

dynamical motion as dynamical behavior which is sensitive to small differences in the initial injection conditions and which results in chaotic motion within a restricted domain, one can see from the studies reported in this paper that the SSC is characterized by bounded chaotic behavior. The dynamic aperture is the spatial region throughout which the beam operates and beyond which particle motion becomes unstable and results in unacceptable particle loss. The agreed recommended safe dynamic aperture radius for the Collider is 4 mm. This represents a distance of 10 standard deviations of the rms beam radius at injection. It is seen from these studies that the 4 cm magnetic aperture design is unsafe with respect to plausible magnetic multipole errors which lead to erratic dynamical motion as a result of the nonlinearities they introduce into the magnetic field.

During the injection period into the Collider the proton beams must be stable for up to 7.0×10^6 turns. This corresponds to approximately 40 minutes. Numerical simulations of this process have been performed to observe the dynamical behavior of particles tracked through the Collider. In this paper, three long term tracking runs are described and their results are reported. A particle is determined to be lost if its distance from the closed orbit exceeds $\sqrt{2}$ 15 mm during a drift between thin elements. The number of turns before a particle is lost has been recorded against initial injection amplitude, and these graphs are shown. In addition, the maximum values of the x and y invariant amplitudes averaged over 10^4 turns are presented. The results have been obtained using the code SSCTRK. Plausible multipole errors have been introduced to simulate the expected realistic levels which can be measured. These errors and other assumptions regarding the plausible machine have been described in these proceedings by T. Garavaglia, K. Kauffmann and R. Stiening in Ref. 1.

SSCTRK

SSCTRK is a FORTRAN 77 code for the numerical simulation of particle tracking within the SSC lattice. There are versions which can be run on Sun workstations, IBM, Cray, and SX-2 supercomputers. The supercomputer version for the Cray is a vectorized code with inner DO loops written in assembly language to enhance the running speed. The Cray version can track up to 64 particles simultaneously. It has been used to track particles in a plausible machine of 4 cm aperture for seven million turns and in a plausible machine of 5 cm aperture for three million turns. Data on the $|i_x|$, $|i_y|$ values, and $(|i_x|^2 + |i_y|^2)^{1/2}$ values where $|i_x| = (x^2 + (\alpha_x + \beta_x\theta)^2)^{1/2}$ and where $|i_y| = (y^2 + (\alpha_y + \beta_y\theta)^2)^{1/2}$ for the usual α and β of betatron oscillations can be extracted at each element. Also information regarding the lifetime of a particle as well as smear information can be obtained. Typically data are taken and averaged over 10,000 turns for runs of more than 3 million turns. In addition, the values of x' and y' have been used to make phase space plots. In a typical long run, four particles are injected with equal x and y values on four different grid points for one of eight possible random seeds, each seed

representing the simulation of a different machine, which represent the various random errors associated with the multipoles.

LONG TERM TRACKING

The results for three cases, Figures 1 through 5 (RUN50), Figures 6 through 10 (RUN58), and Figures 11 through 13 (RUN68), are presented. The first and last are simulations of the SSC with a 4 cm magnetic aperture, and the second is a simulation with a 5 cm magnetic aperture.

RUN50: 4 cm Magnet

Chromaticity corrections in x and y have been made; however, a 3.75% error is introduced in the setting of the chromaticity sextupoles. This is equivalent to an error of about 5 units. Systematic multipole errors appropriate for a 4 cm magnet have been assumed. The quadrupole persistent current duodecapole error has been suppressed. All multipoles have a systematic value of 0.05 units except the regular sextupole, the regular quadrupole, and the skew quadrupole. This level is viewed as the limit of measurement. No ripple has been introduced, and a momentum error of 5×10^{-4} has been used. The momentum error is achieved by injecting with no dp/p but with a 16.4 cm error in z_0. Four particles where started on a grid of 2, 3, 4, and 5 mm in eight different machines. This run had the same input information as a previous 10^5 turns simulation, RUN25 of Ref. 1; however, particles where tracked for 7×10^6 turns. As is usual, when a particle is lost another is started at a grid point that has been stepped in by one grid unit from the starting position of the one which was lost.

The results of this run can be seen in Figure 1 where a dynamic aperture of between 3 and 4 mm is seen. This is to be compared with the result of RUN68 in Figure 11 where a finer grid was used. This figure indicates an aperture of approximately 3.5 mm. Graphs for particles started at four different equally spaced grid points are given for the x and y invariant amplitudes as a function of turns for two representative random seeds. The results for RUN50 are given in Figures 2 through 5. It is clear that nonlinear dynamical behavior is seen at 3 mm and above. In addition, one can see in comparing the graphs for the x and y invariant amplitudes, e.g. Figures 2 and 3, a clear cross coupling where the y behavior is an approximate reflection symmetry of the x behavior; however, the x and y invariant amplitudes can be driven to different maximum values.

RUN58: 5 cm Magnet

This is an example where the multipoles have been chosen which are appropriate for a 5 cm magnet. The quadrupole persistent current duodecapole has been suppressed. All multipoles have a systematic value of 0.05 units except for the regular sextupole, regular quadrupole, and skew quadrupole. This level is viewed as the limit of measurement. The momentum error associated with

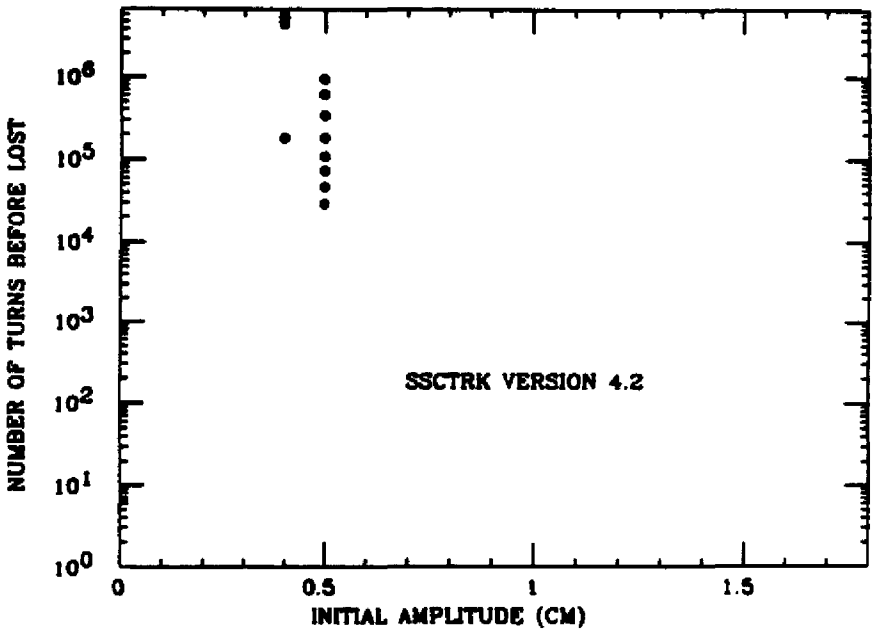

Figure 1. Particle Lost Run = 50

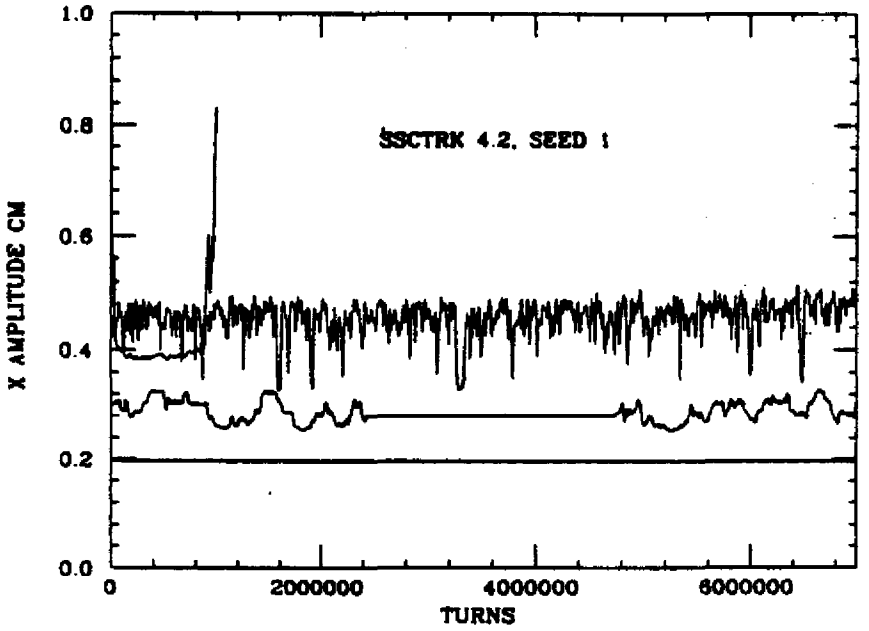

Figure 2. X vs. Turns Run = 50 4 cm Magnet

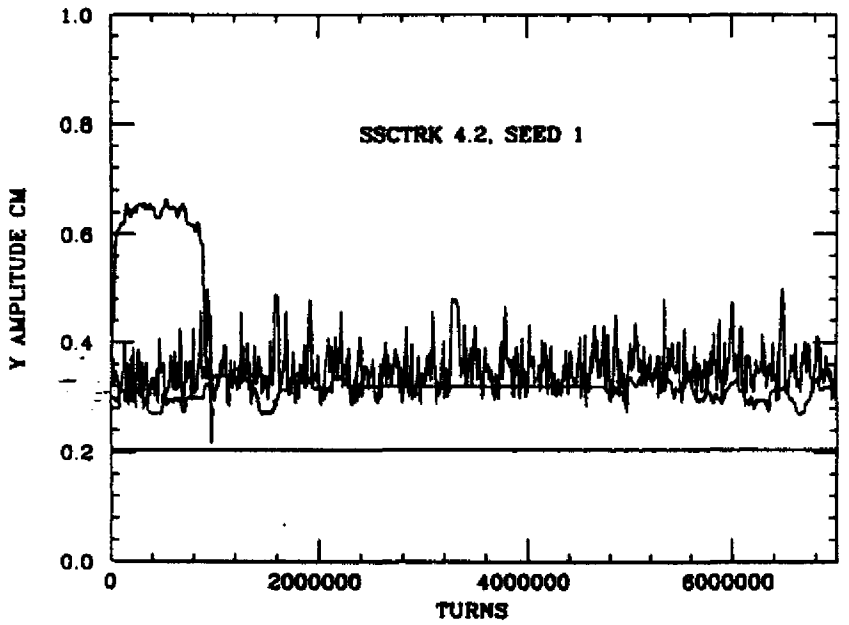

Figure 3. Y vs. Turns Run = 50 4 cm Magnet

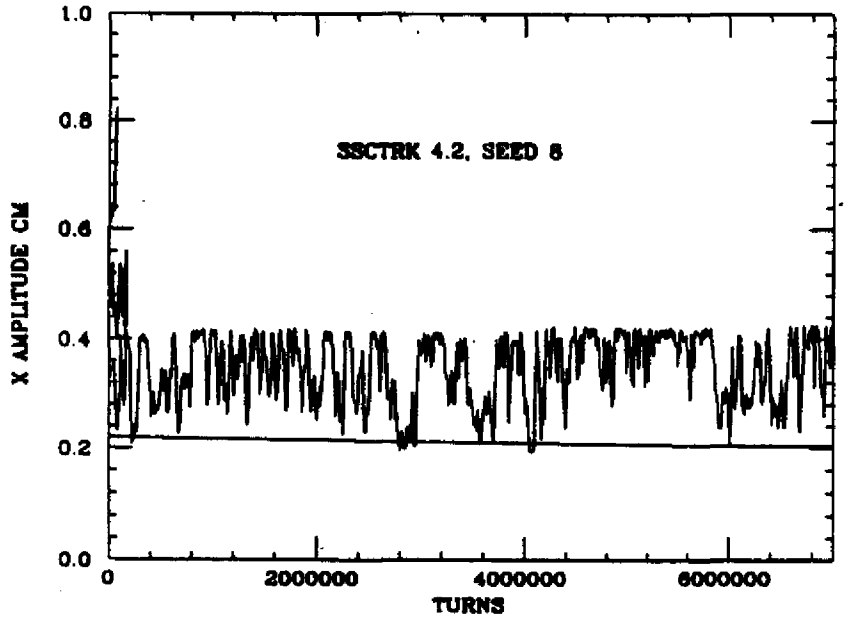

Figure 4. X vs. Turns Run = 50 4 cm Magnet

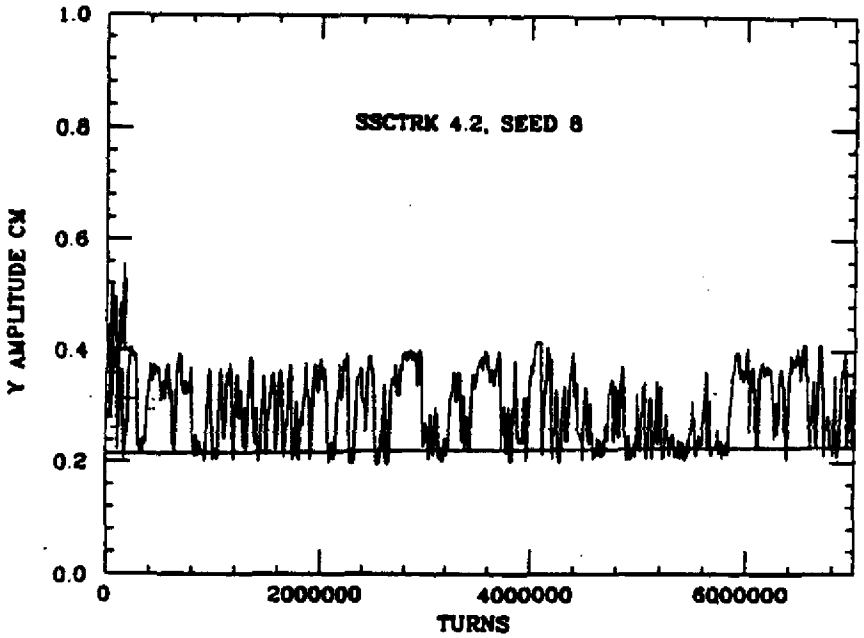

Figure 5. Y vs. Turns Run = 50 4 cm Magnet

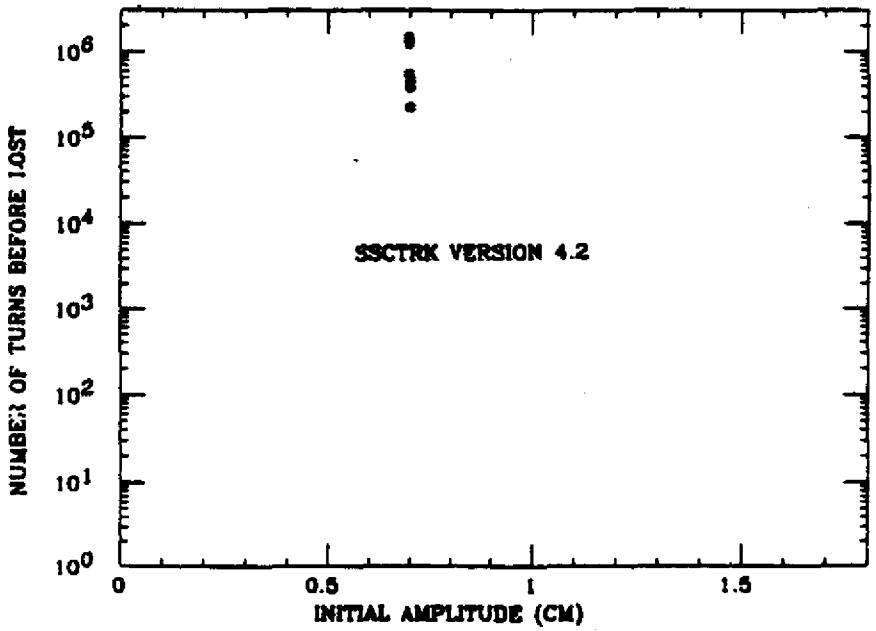

Figure 6. Particles Run = 58

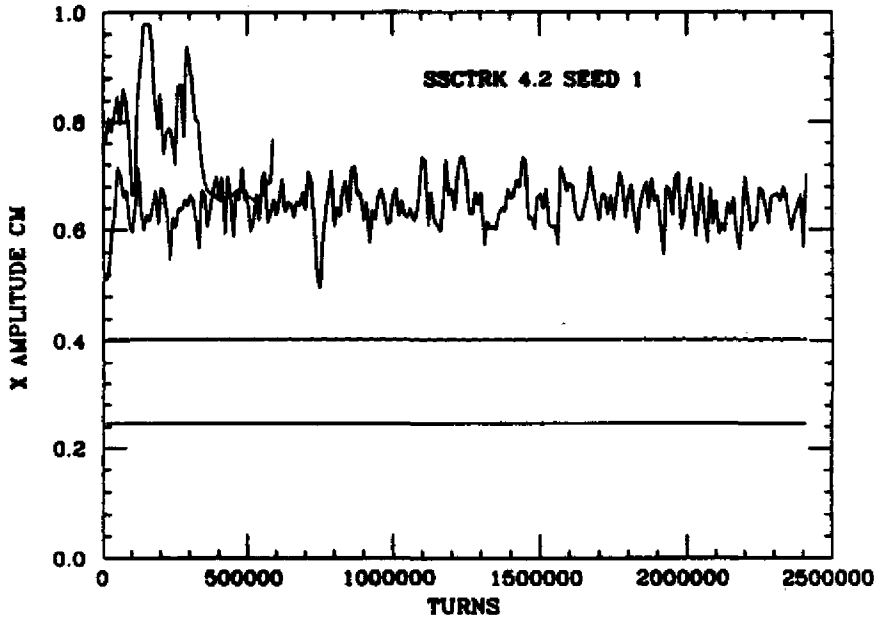

Figure 7. X vs. Turns Run = 58 5 cm Magnet

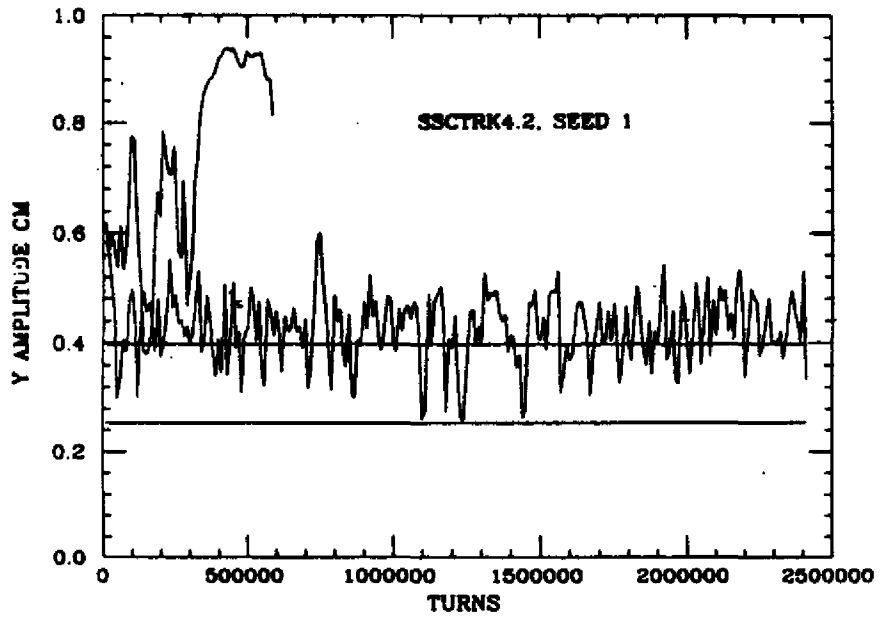

Figure 8. Y vs. Turns Run = 58 5 cm Magnet

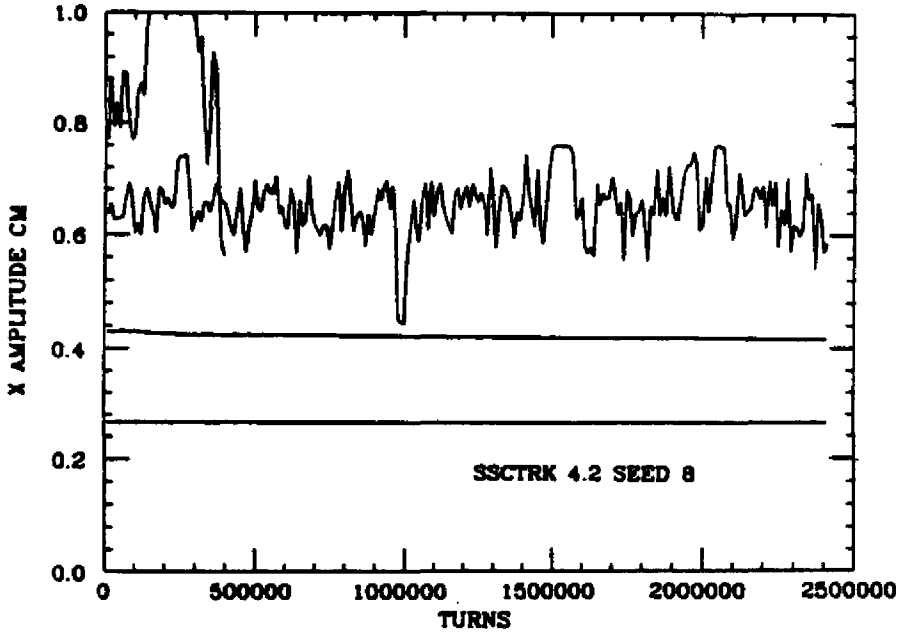

Figure 9. X vs. Turns Run = 58 cm Magnet

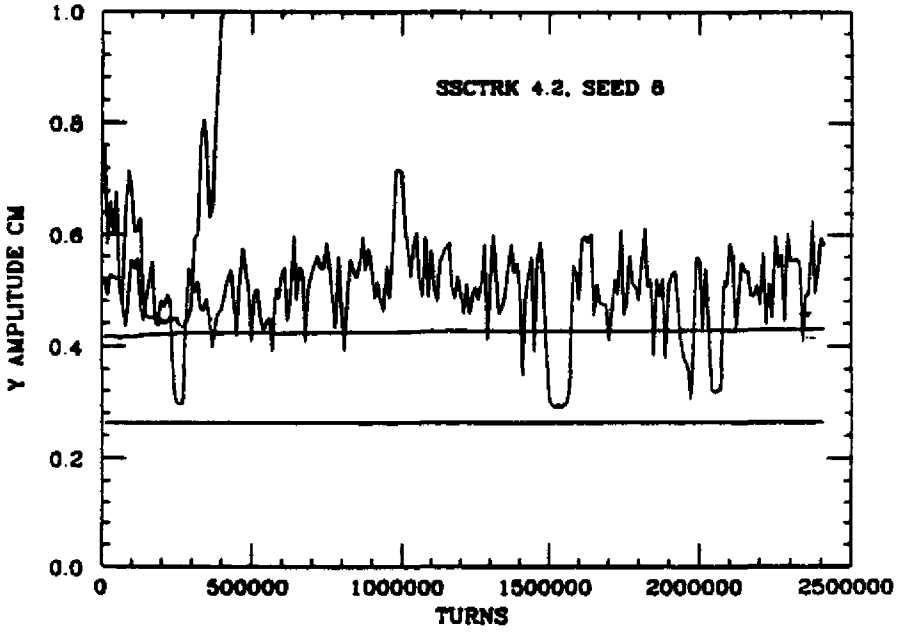

Figure 10. Y vs. Turns Run = 58 cm Magnet

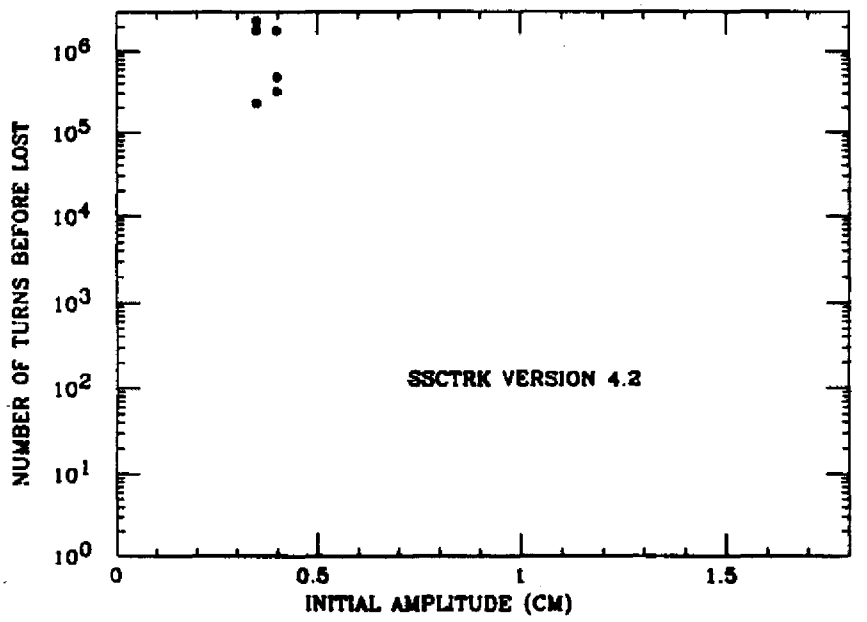

Figure 11. Particles Lost Run = 68

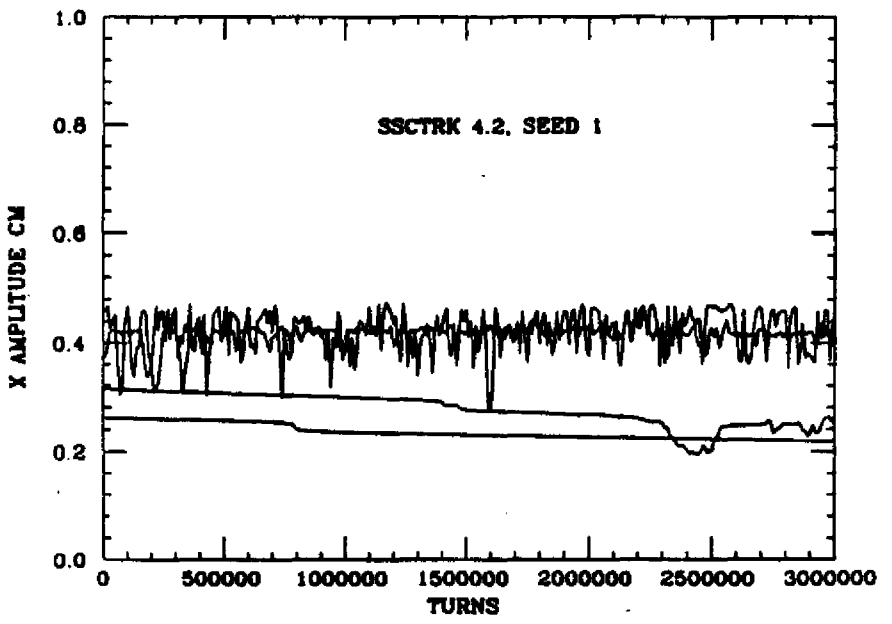

Figure 12. X vs. Turns Run = 68 4 cm Magnet

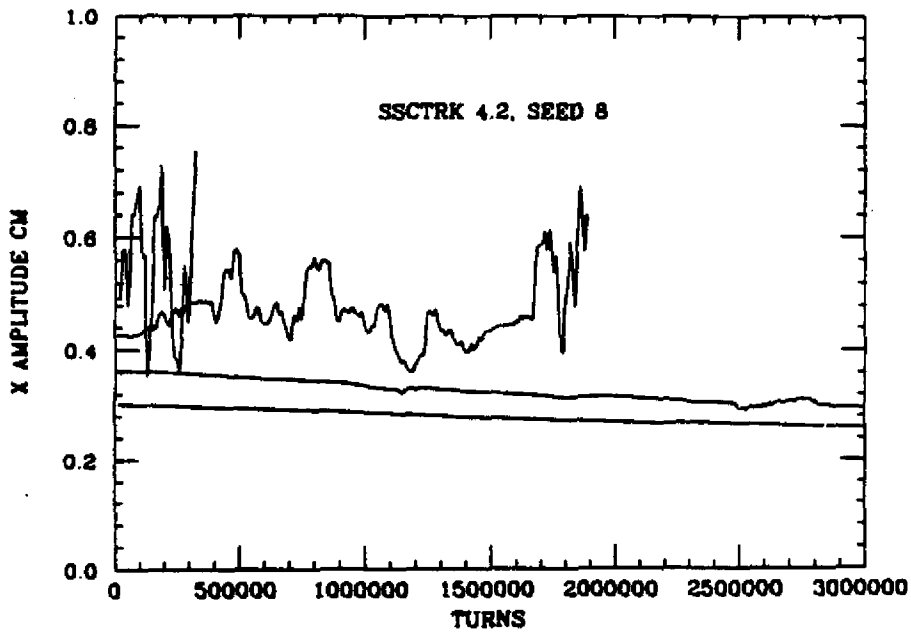

Figure 13. X vs. Turns Run = 68 4 cm Magnet

synchrotron oscillations is 5.0×10^{-4}. This has been achieved with $dp/p = 0$ and a 16.4 cm z_o error. This is the same as RUN36 which is discussed in Ref. 1; however, it has been run for 3×10^6 turns. Particles where injected at 2.5, 4.0, 5.5, and 7.0 mm into eight different machines. Figure 6 shows an aperture of approximately 5.2 mm. In addition, the x and y invariant amplitude graphs for this run, given in Figures 7 through 10, show particles running stably at 4 mm. Here one sees the usual xy coupling and the presence of nonlinear effects beyond 5.5 mm.

RUN68: 4 cm Magnet

Particles where tracked in this run for 3×10^6 turns with the multipoles appropriate for the 4 cm magnet. This is basically the same as RUN50; however, particles were injected into the eight machines on a finer grid at the points 2.5, 3.0, 3.5, and 4.0 cm. It is seen from Figure 11 for the number of turns before a particle was lost that the dynamical aperture is approximately 3.5 mm. In addition, and inspection of the graphs for the x and y invariant amplitudes as a function of turns, Figures 12 and 13, demonstrates the usual irregular nonlinear behavior of the amplitudes.

BOUNDED CHAOTIC MOTION: **Figures 14 through 16 (RUN681)**

RUN681 has the same run card as Figures 14 through 16 (RUN68); however, two particles where started at nearby points and tracked using seed 1 for

10^6 turns on a Cray 2 machine. Particle one was started at 3.5 mm and particle two was started at $3.5 + 10^{-10}$ mm. Graphs where made of the value of the modulus, $(|i_x|^2 + |i_y|^2)^{1/2}$ of the two particles as a function of turn number. These are shown in Figures 14 and 15, respectively. The Euclidean distance between the two particles as a function of turn number is given in Figure 16. It is clear from Figure 14 that a bifurcation takes place after 15,000 turns. Figure 15 shows that bounded chaotic motion persists for the full 10^6 turns. Furthermore, Figure 16 shows that the long term growth of the Euclidean distance between the points, $\sqrt{(|i_{x2}| - |i_{x1}|)^2 + (|i_{y2}| - |i_{y1}|)^2}$, is neither Lyapunov exponential nor diffusive, i.e. growing as $(\sqrt{\text{time}})$.

In addition to the x and y invariant amplitude figures already discussed, one can see the nature of the chaotic behavior of the dynamical motion of the particle injected at 3.5 mm from phase space figures for both (x, x') and (y, y'). These are seen in Figures 17 and 18 where the phase space points are filling an annulus. The skew symmetry between these two figures is the result of x and y coupling.

QUALITATIVE BEHAVIOR

A certain qualitative understanding of the results presented above for the nonlinear dynamical behavior of the particles during the long term tracking simulations can be obtained from the study of a simple model using nonlinear differential equations of the type

$$x'' + \omega^2 x = d_3 x^2 + d_4 x^3 + e_{11} xy + e_{12} xy^2 + \text{etc.} + F_{random}$$
$$y'' + \omega^2 y = d_3 y^2 + d_4 y^3 + f_{11} xy + f_{12} xy^2 + \text{etc.} + F_{random}$$

which are solved numerically using the CERN Programme Library Runge-Kutta integration routine RKSTP. For this system, x space and phase space plots show how a particle can be lost when it is near the separatrix. Also one can see how a random force can cause particle loss. Furthermore, one can study the effects of coupling, and one can simulate the behavior seen in Figure 2 for the long term tracking study where the invariant amplitude can make transitions between large and small average values.

For stable motion, with $\omega = 2$ and with only d_4 nonzero, the amplitude as a function of time behaves as shown in Figure 19. The associated phase space portrait shown in Figure 20 determines the separatrix for this system. If the parameter in this system is changed from $d_4 = 8.0007910$ to the value $d_4 = 8.0007911$, the result can be seen in Figures 21 and 22 for the amplitude and phase space behavior where the particle becomes unstable upon crossing the separatrix. This represents a dynamical behavior that can account for particle loss. As a further illustration, a Gaussian random force has been applied to this equation and the results on stable motion can be seen in Figures 23 and 24 for the amplitude and phase space behavior respectively. Here one clearly sees how a random force can cause the particle to cross the separatrix and

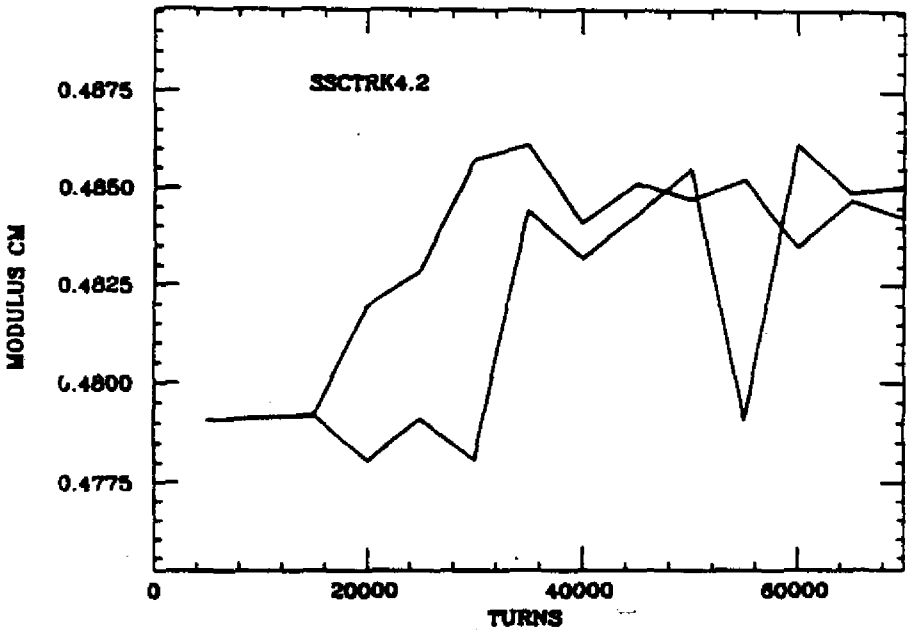

Figure 14. Mod 1 and 2 vs. Turns Run = 681 Chaos

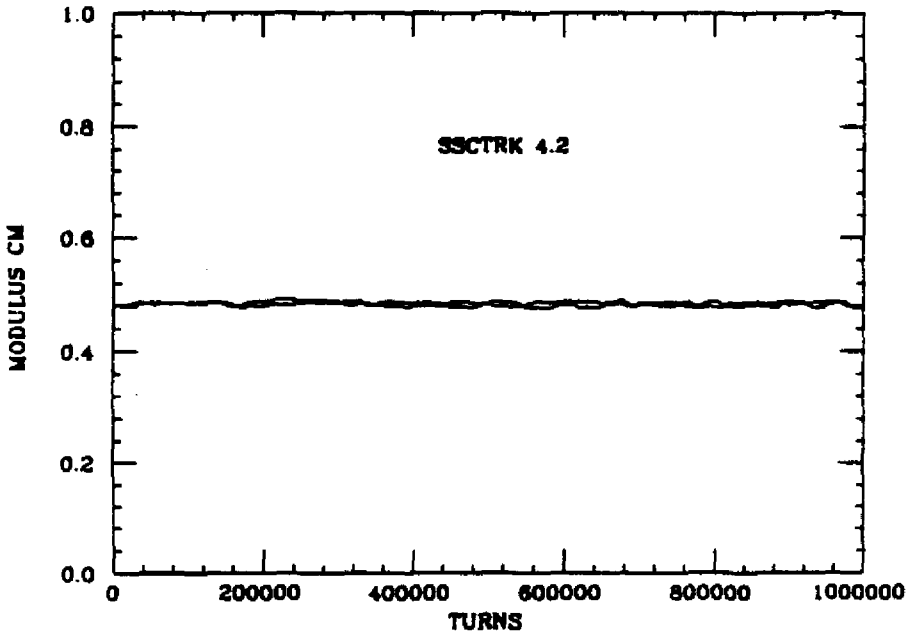

Figure 15. Mod 1 and 2 Turns Run = 681 Chaos

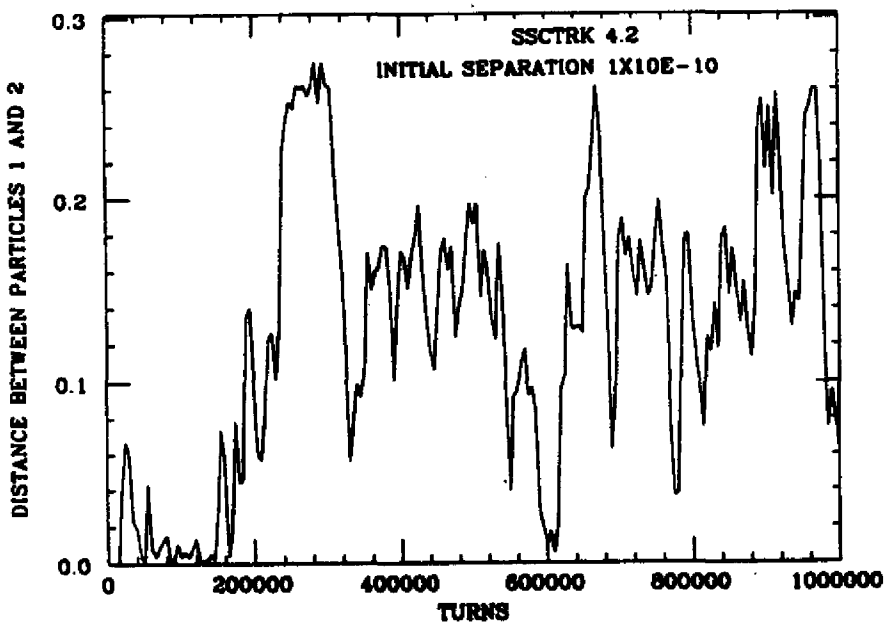

Figure 16. Initial Separation $1 \times 10E^{-10}$

become lost. In addition, Figure 23 shows that the random force has an effect on the magnitude of the amplitude, and Figure 24 shows chaotic motion in phase space before the separatrix is crossed. It is possible to simulate the cross coupling behavior similar to that seen in the long term tracking results when the system of nonlinear differential equations for the x and y amplitudes are solved numerically and when this system is cross coupled with terms of the form xy, x^2y, y^2x, etc., which occur in multipole expansions. If both the x and y systems are started with the same initial conditions, one can see how a simple xy coupling introduced in the equation for x can drive the y amplitude. These results are represented in Figures 25 and 26 where $y1$ and $y2$ denote the x and y amplitudes, respectively. In this example there is no random force, and the nonzero parameters have the values $\omega = 2$, $d_3 = 0.5$, $d_4 = 7.000791$, and $f_{11} = 1$.

As a final remark, it is worth noting that behavior where the amplitude makes a transition between different values after a large number of turns is a characteristic of nonlinear driven differential equations. This results when the amplitude becomes a multivalued function of the driving frequency. This can result in a transition in the value of the amplitude. An example of this behavior is seen in Figures 2, 3, 27, and 28. The first two figures result from SSCTRK, and the last two figures are found from the first differential equation of the system already considered. The nonzero parameters have the values $\omega = 2$, and $d_4 = 0.1$, and the random force has been replaced with the driving force $0.909\sin(4t + 0.08t^2)$. The amplitude transition seen in Figure 27 occurs after

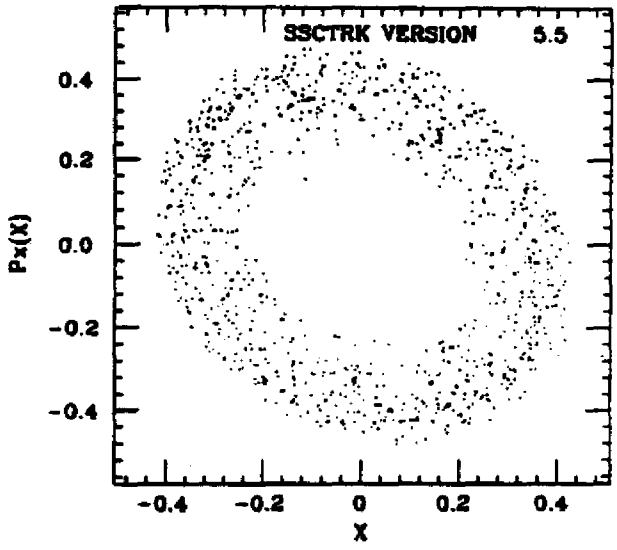

Figure 17. X Phase Space Plot Run = 68

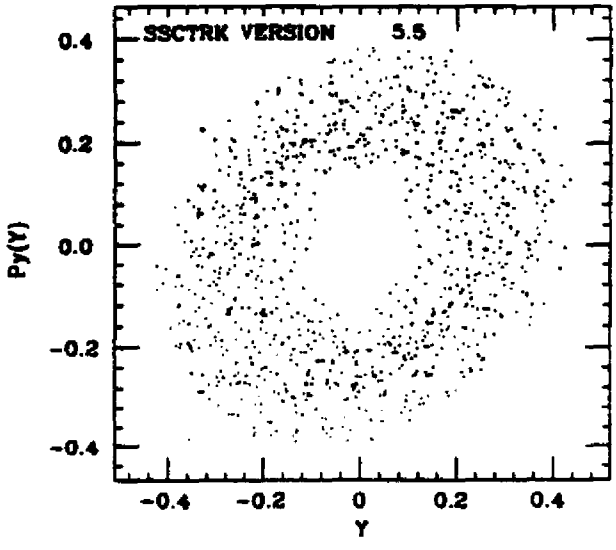

Figure 18. Y Phase Space Plot Run = 68

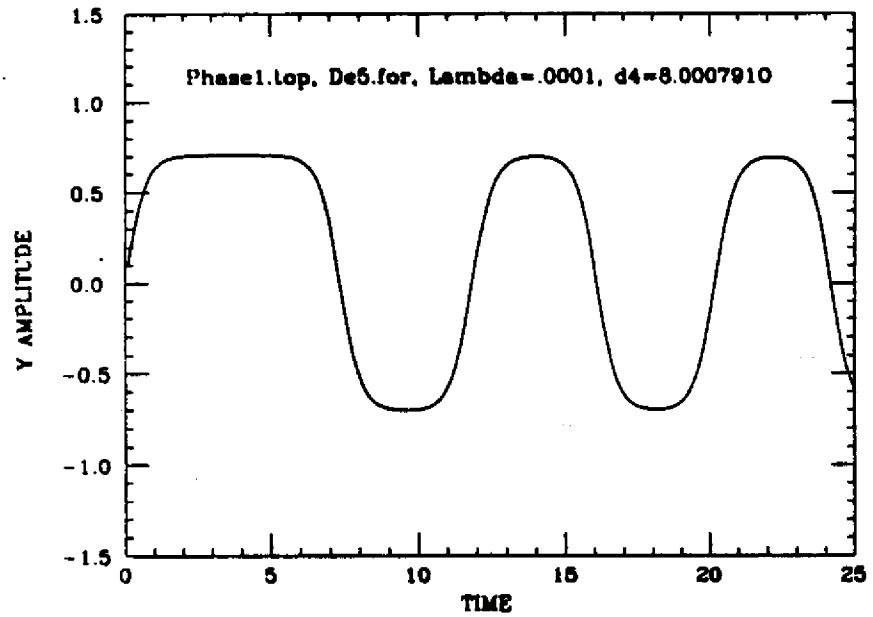

Figure 19. Amplitude vs. Time 1

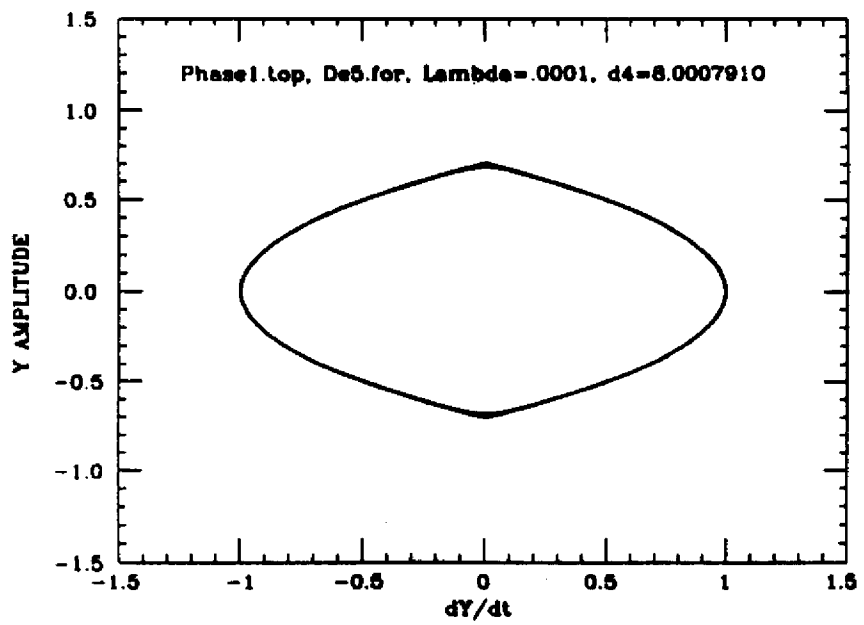

Figure 20. Phase Space 1

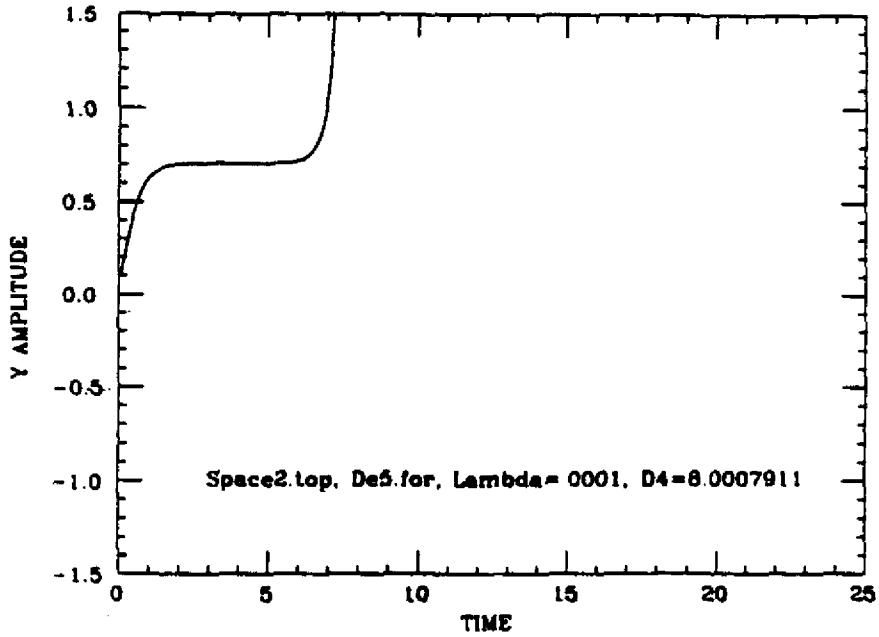

Figure 21. Amplitude vs. Time 2

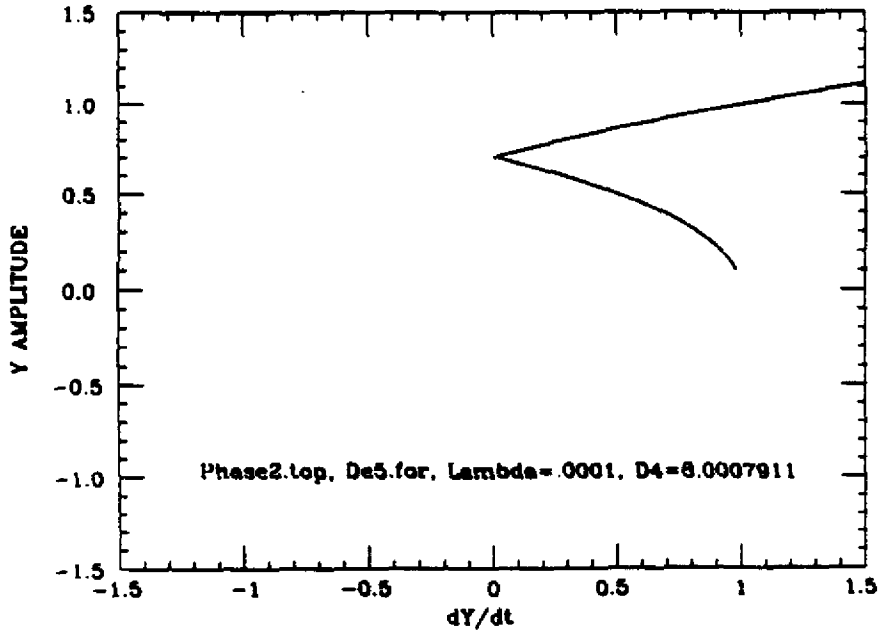

Figure 22. Phase Space 2

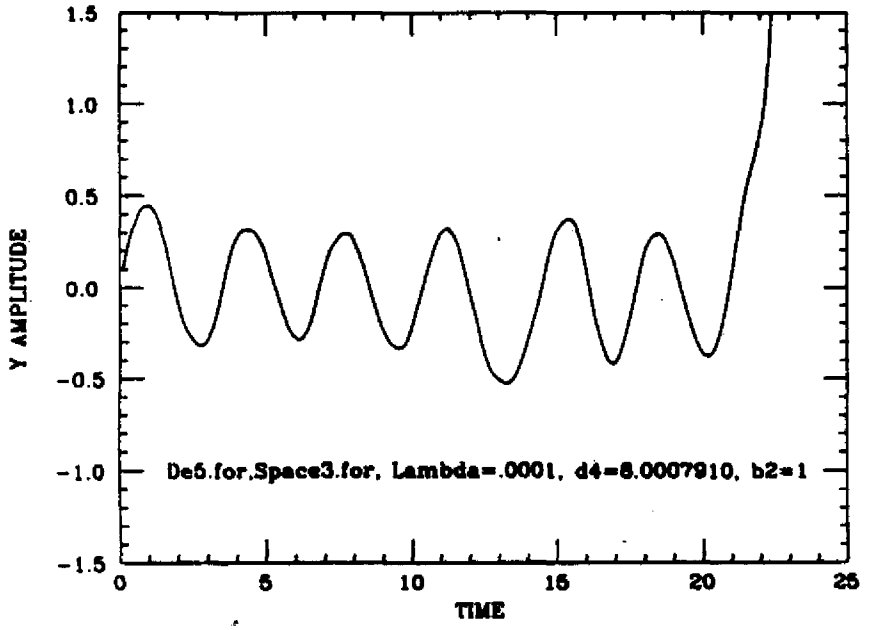

Figure 23. Space 3

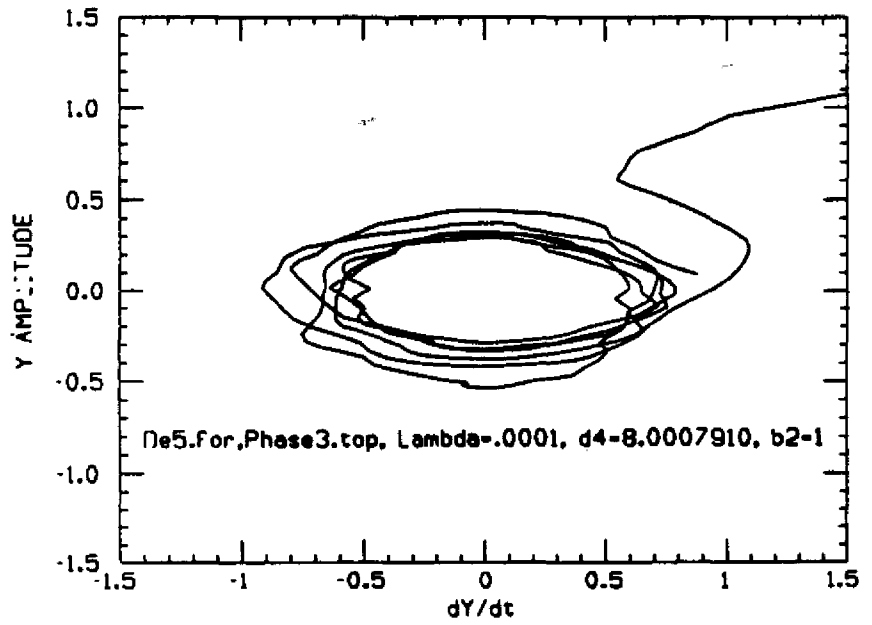

Figure 24. Phase Space 3

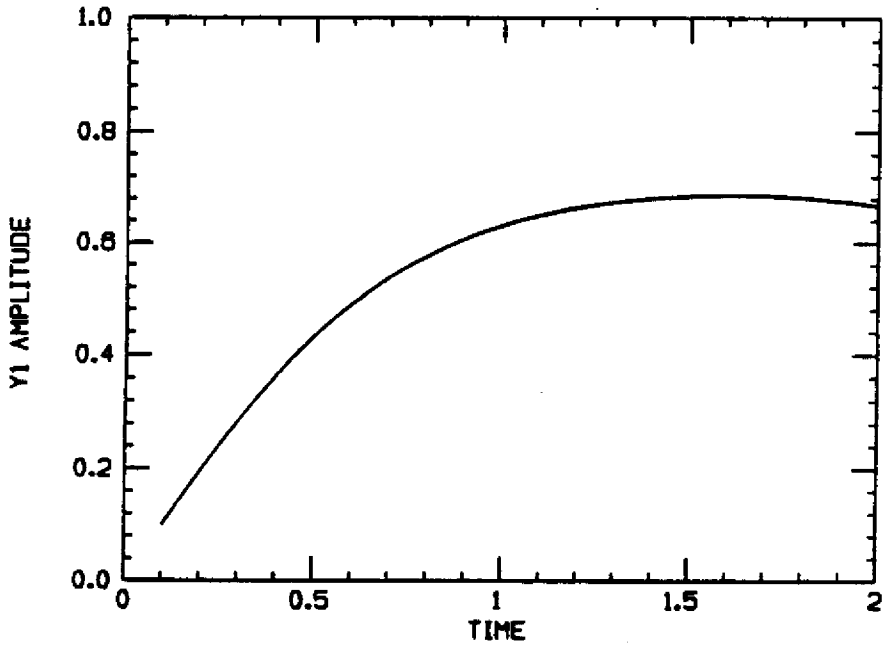

Figure 25. Space 4A

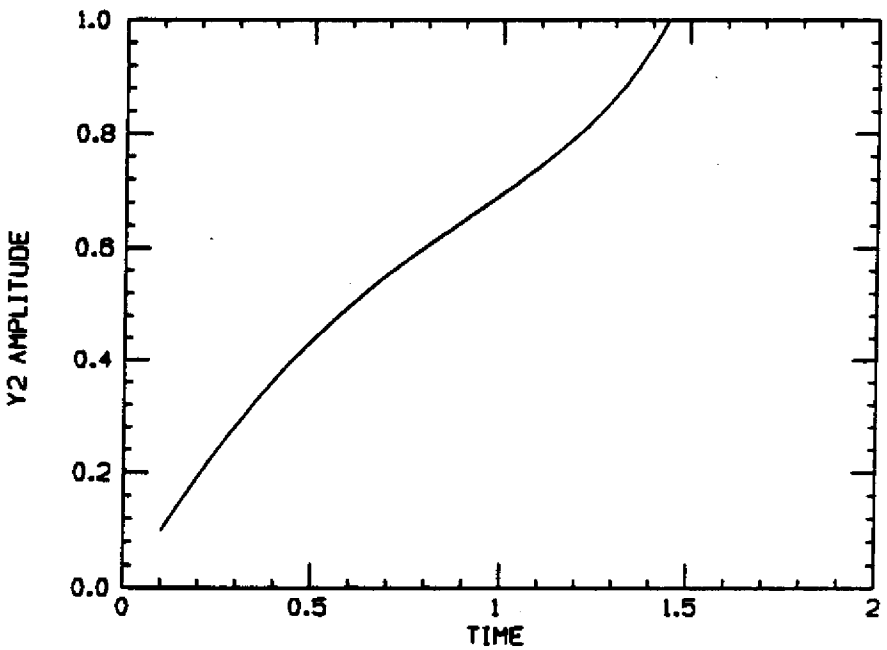

Figure 26. Space 4B

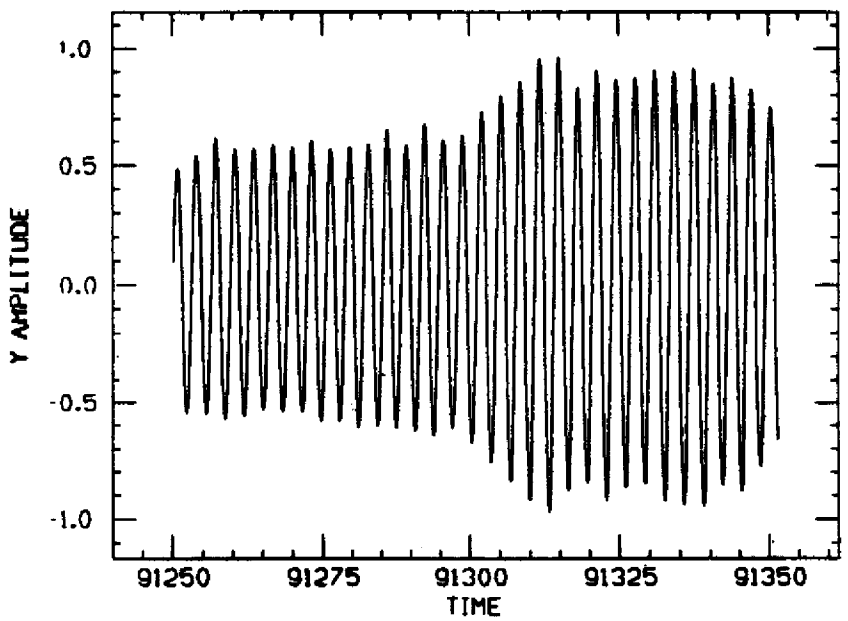

Figure 27. Space 7.FOR

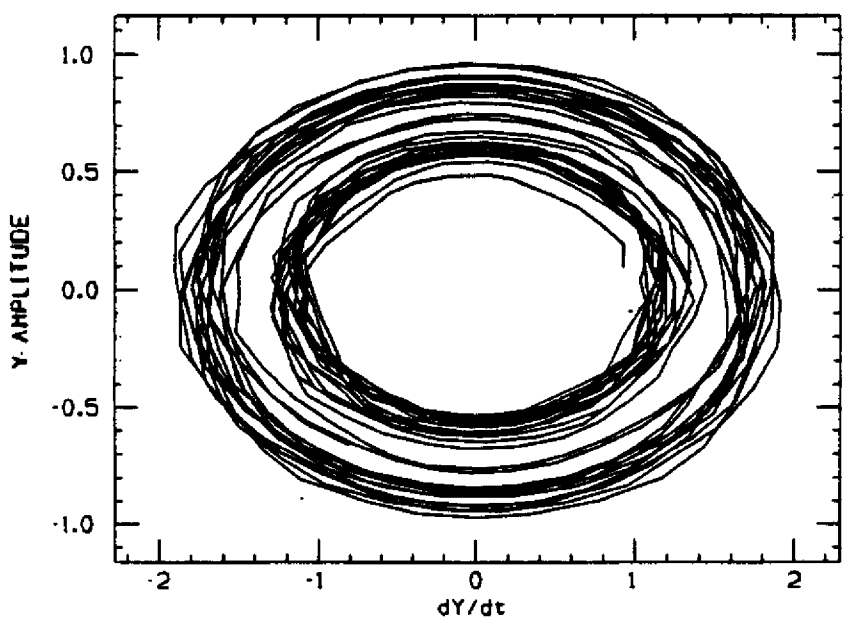

Figure 28. Phase Space 7

a large number of cycles, and the phase space graph in Figure 28 shows chaotic motion and transition regions. A further discussion of this phenomenon can be found in Refs. 3 and 4.

Although the system of differential equations used to produce the above results is much simpler than the tracking code SSCTRK, it does provide a qualitative understanding of the origin of the dynamical behavior seen in the long term tracking studies. Furthermore, the inclusion of random multipole errors in the tracking code does appear to have the effect of producing random forces characterized by mixtures of harmonics which can drive particles across a separatrix or produce transitions in the magnitude of oscillation amplitudes.

References

1. T. Garavaglia, S. K. Kauffmann, and R. Stiening, Collider Ring Particle Loss Tracking With SSCTRK, in: "International Industrialization for the Superconducting Super Collider (IISSC) Proceedings" (1990).
2. H. Mais, G. Ripken, and A. Wrulich, Particle Tracking, in: "CERN Accelerator School CERN 87-03," S. Turner, ed., CERN, Geneva (1987).
3. J. M. Jowett, M. Month, and S. Turner, Nonlinear Dynamics Aspects of Particle Accelerators, in: "Lecture Notes in Physics 247," Springer-Verlag, Heidelberg (1986).
4. E. A. Jackson, "Perspectives of Nonlinear Dynamics," Cambridge University Press, Cambridge (1986).